HHS Public Access

Author manuscript

J Immunol. Author manuscript; available in PMC 2022 July 01.

Published in final edited form as:

J Immunol. 2021 July 01; 207(1): 101–109. doi:10.4049/jimmunol.2001363.

pH and proton sensor GPR65 determine susceptibility to atopic dermatitis

Liang Xie[*,†], **Craig I. Mckenzie**[‡,§], **Xinyan Qu**[¶], **Yan Mu**[¶], **Quanbo Wang**[¶], **Nan Bing**[||], **Karmella Naidoo**[#], **Md Jahangir Alam**[*], **Di Yu**[¶,**], **Fang Gong**[††], **Caroline Ang**[‡‡], **Remy Robert**[§§], **Francine Z. Marques**[†,¶¶], **Nicholas Furlotte**[|| ||], **David Hinds**[|| ||], **Olivier Gasser**[#], **23andMe Research Team**[|| ||], **Ramnik J. Xavier**[##,***,†††], **Charles R. Mackay**[*,¶,1]

[*] Department of Microbiology, Biomedicine Discovery Institute, Monash University, Clayton, VIC 3800, Australia

[†] Hypertension Research Laboratory, School of Biological Sciences, Monash University, Clayton, VIC 3800, Australia

[‡] Department of Immunology and Pathology, Central Clinical School, Monash University, Melbourne, VIC 3004, Australia

[§] Department of Allergy, Immunology and Respiratory Medicine, Central Clinical School, Monash University, Melbourne, VIC 3004, Australia

[¶] School of Pharmaceutical Sciences, Shandong Analysis and Test Center, Qilu University of Technology (Shandong Academy of Sciences), Jinan, 250014, China

[||] Pfizer Inc, Cambridge, MA, 02139, USA

[#] Malaghan Institute of Medical Research, Victoria University of Wellington, Wellington 6012, New Zealand.

[**] The University of Queensland Diamantina Institute, Faculty of Medicine, The University of Queensland, Brisbane, QLD 4102, Australia

[††] Department of Laboratory Medicine, Wuxi Hospital of Integrated traditional Chinese and Western Medicine, Affiliated Hospital of Jiangnan University, Wuxi, 214041, China

[‡‡] Department of Biochemistry and Molecular Biology, Biomedicine Discovery Institute, Monash University, Clayton, VIC 3800, Australia

Correspondence: charles.mackay@monash.edu (C.R.M.), Phone: +61 03 99050646.

[1]Lead Contact

Author contributions

L.X. planned and performed most of the experiments and wrote the manuscript. C.I.M planned and performed mouse *in vitro* experiments. X.Q., Y.M., Q.W. planned and performed human study. N.B. planned and performed PheWAS. K.N. and M.J.A. performed animal experiments. D.Y. and F.G. provided samples for human study. C.A. performed animal experiments. R.R. and F.Z.M. discussed mechanistic concepts and edited manuscript. N.F., D.H. performed analysis for PheWAS. O.G. discussed mechanistic concepts and edited manuscript. R.J.X. discussed mechanistic concepts and edited the manuscript. C.R.M. initiated, supervised the project and wrote the manuscript.

Declaration of interests

N.B. was employed by Pfizer at the time of this research. N.F. and D.H. were employed by 23andMe at the time of this research and hold stock or stock options in 23andMe. Other authors declare no conflict of interest.

§§ Department of Physiology, Biomedicine Discovery Institute, Monash University, Clayton, VIC 3800, Australia

¶¶ Heart Failure Research Laboratory, Baker Heart and Diabetes Institute, Melbourne, VIC 3004, Australia

‖‖ 23andMe, Inc. Sunnyvale, 94086, California, USA

Broad Institute, 02142, Massachusetts, USA

*** Center for Computational and Integrative Biology, Department of Molecular Biology, Massachusetts General Hospital and Harvard Medical School, Boston, 02114, Massachusetts, USA

††† Center for Microbiome Informatics and Therapeutics, Massachusetts Institute of Technology, Cambridge, 02139, Massachusetts, USA

Abstract

pH-sensing by GPR65 regulates various inflammatory conditions but its role in skin remains unknown. Here we performed a phenome-wide association study (PheWAS) and report that the T allele of *GPR65* intronic SNP rs8005161, which reduces GPR65 signaling, showed a significant association with atopic dermatitis, in addition to inflammatory bowel diseases and asthma, as previously reported. Consistent with this genetic association in humans, we show that deficiency of GPR65 in mice resulted in markedly exacerbated disease in the MC903 experimental model of atopic dermatitis. Deficiency of GPR65 also increased neutrophil migration *in vitro*. Moreover, GPR65 deficiency in mice resulted in higher expression of the inflammatory cytokine tumor necrosis factor α (TNFα) by T cells. In humans, $CD4^+$ T cells from rs8005161 heterozygous individuals expressed higher levels of TNFα after PMA/ionomycin stimulation, particularly under pH 6.0 conditions. pH sensing by GPR65 appears to be important for regulating the pathogenesis of atopic dermatitis.

Keywords

pH; GPR65; Phenome-wide association study; epithelial inflammation; atopic dermatitis

Introduction

Extracellular acidic pH occurs in certain epithelia of the colon and skin, and at sites of inflammation [1]. It is sensed by several proton-sensing G-protein coupled receptors (GPCRs), including GPR65, which is widely expressed on immune cells [2]. It signals through Gαs leading to cAMP production, which phosphorylates the transcription factor CREB (cAMP response element-binding protein) and blocks its binding to the NF-κB complex, thus limiting various pro-inflammatory responses [3]. Normal signaling through GPR65 under low pH inhibits the release of inflammatory cytokines from immune cells [4–6]. Furthermore, GPR65 is of great disease significance that GPR65 deficient animals exhibit exacerbated inflammation in pre-clinical models of inflammatory bowel disease (IBD) [7, 8] and acute lung injury [9]. A GPR65 missense variant rs3742704 (I231L)

and a *GPR65* intronic SNP rs8005161 are among the top variants associated with the risk of human IBD (both ulcerative colitis and Crohn's disease) in multiple studies [10–13]. Together pH and GPR65 signalling may be a major mechanism for the regulation of inflammation, particularly at the epithelia.

Atopic dermatitis (AD) is a chronic and relapsing inflammatory skin disease characterized by intense pruritic and eczematous lesions. AD affects 15–30% of children and 2–10% of adults in western societies [14]. Mechanisms thought to underlie AD pathogenesis include both excessive type 2 inflammatory responses and impairment of barrier function [15, 16]. While AD is highly heritable [17, 18], findings of the existing genome-wide association studies (GWASs) only account for ~30% of AD heritability [19, 20]. Regulation of skin pH may be an overlooked important factor. The surface pH of healthy skin is typically 4.5–6 [21]. AD lesions have been reported to show higher pH values than healthy skin, and pH was positively associated with the severity of AD [22, 23]. In a mouse model of AD, exposure to alkaline agents increased the severity of dermatitis lesions, while topical application of acids improved skin barrier function [24–26]. However, the role of pH-sensing by GPR65 in skin remain unknown.

In this study, we performed a phenome-wide association study (PheWAS) for *GPR65* intronic SNP rs8005161 to understand the broader disease significance of GPR65 in human health. Apart from the known association with IBD, the minor T allele of rs8005161 was found to be strongly associated with human AD. In alignment with this, the absence of GPR65 in mice ($GPR65^{gfp/gfp}$) led to exacerbated skin inflammation in an experimental AD model, with significant elevation of skin pH. Furthermore, the exacerbated AD in $GPR65^{gfp/gfp}$ mice was characterized by increased infiltration of various types of immune cells. $Gpr65^{gfp/gfp}$ neutrophils showed changes in cell migration properties, *in vitro*. In addition, mouse $Gpr65^{gfp/gfp}$ T cells and human rs8005161-CT T cells showed increased production of the AD pathogenic cytokine tumor necrosis factor α (TNFα) [27]. Together, these data highlight a critical role of GPR65 in leukocyte migration, cytokine responses, and the pathogenesis of AD in mice and humans.

Materials and Methods

Phenome-wide association studies of GPR65 SNP rs8005161

Phenome-wide association study (PheWAS) was conducted in the 23andMe participant cohort from 647,776 participants of European ancestry. A total of 1,228 phenotypes collected within 23andMe's data were included for exploration. Phenotype data are derived from responses to self-reported questionnaires. The association of rs8005161 with each phenotype was evaluated using a likelihood ratio test comparing the full model against null model with or without genotype adjusted for age, gender, genotyping array design, and PCs to correct for population stratification. Binary phenotypes were analyzed using logistic regression, quantitative phenotypes were analyzed using linear regression and survival phenotypes were analyzed using Cox proportional hazard regression. We assume additive allelic effects. False Discovery Rate (FDR) for each phenotype was calculated using the Benjamini-Hochberg procedure.

Mice

All experimental procedures involving mice were carried out according to protocols approved by the Animal Ethics Committees of Monash University and Victoria University of Wellington. *Gpr65*$^{gfp/gfp}$ mice were purchased from Jackson labs (stock number 008577). *Gpr65*$^{gfp/gfp}$ mice have 90% of exon 2 coding sequences are replaced by promoterless IRES-EGFP sequences to disrupt GPR65 function [28]. WT controls were C57BL/6 mice obtained from the Monash Animal Research Platform, Monash University. All mice were maintained under specific pathogen free and controlled environmental conditions.

MC903 treatment of mice

Mice were anaesthetized using isoflurane. MC903 (calcipotriol; Cayman Chemicals, Ann Arbor, MI) was dissolved in 100% ethanol and topically applied on mouse ears (1nmol in 20μl, 10μl per side of ear) on days 0, 2, 5, 7, 9, 12, 14. As vehicle control, the same volume of ethanol was applied. All experiments were performed on age- and sex-matched animals.

TEWL measurement

TEWL was measured while mice were sedated, using the DERMALAB TEWL probe (Cortex Technology, Hadsund, Denmark) at endpoint. TEWL was measured on both ears of the mice at room temperature, and results were recorded when TEWL regions stabilized. Two readings from each ear were taken and averaged for each mouse.

Skin pH measurement

Skin pH was measured while mice were sedated, using the skin & scalp pH meter (Hanna Instruments, USA) on day 14. Skin pH was measured on both ears of the mice at room temperature, and results were recorded when pH regions stabilized. Two readings from each ear were taken and averaged for each mouse.

Itching frequency

Mice were recorded via time-lapse videography, and itch events were determined and quantified. This pathophysiological measurement was obtained from video observation of the relevant treatment groups 24 hours before experimental endpoint.

Histological evaluation and quantification

Ear tissue was fixed in 10% neutral buffered formalin for 24 hours, processed, paraffin embedded, and sectioned at 4 μm. Hematoxylin and eosin (H&E) staining was conducted on ear sections. H&E stained was evaluated at 20x magnification and measurements of acanthosis (epidermal thickening) and dermal thickening were quantified by Image J analysis (National Institutes of Health, Bethesda, MD). Images of the tissue sections were taken on an Olympus IX71 inverted bright-field/fluorescence microscope with an Olympus DP70 digital camera (Olympus, Tokyo, Japan).

Identifying healthy individuals holding the T allele of SNP rs8005161

The human study was reviewed and approved by the human ethics committee of Wuxi Hospital of Integrated traditional Chinese and Western Medicine. The study population

included 189 healthy subjects with Chinese Han ancestry. All subjects provided written informed consent to be included in the study. Genotyping of SNP rs8005161 was performed by DNA sequencing. Briefly, genomic DNA was extracted from buccal swab by TIANamp Swab DNA kit (TIANGEN, Beijing, China). The target DNA was amplified by polymerase chain reaction (PCR) by a PTC-200 PCR instrument (Bio-Rad, Hercules, CA) using the following cycling conditions: 5 minutes at 96°C, 10 cycles of 96°C for 20s, 62–52°C touchdown for 20s, 72°C for 30s, 35 cycles of 96°C for 20s, 52°C for 20s, 72°C for 30s, and 5 mins at 72°C. The amplified DNA were sequenced by an ABI3730XL DNA analyser (Applied Biosystems, Foster City, CA) using the forward primer. The primers used for PCR and sequencing are, Forward: TAAAGGAGGCAAAATAAT, Reverse: CTTCTTTGTAGTGACGCA. 8 subjects carrying rs8005161-CC and 6 subjects carrying rs8005161-CT provided blood samples for the cytokine detection from T cells. Demographic data were obtained at the time of blood collection.

Isolation of mouse immune cells from different tissues and human PBMCs

For mouse skin cell suspensions, ear tissue was split into dorsal and ventral layers and was minced in 2ml RPMI-1640 (Gibco by Life Technologies, Grand Island, NY) with 10% FCS. The tissue was then digested with 2mg/mL Collagenase Type IV (Gibco by Life Technologies, Grand Island, NY) and 120μg/mL DNase I (Roche Diagnostics, Mannheim, Germany) for 20 minutes at 37 °C under agitation. After the digestion, the remaining tissue was passed through a 70-μm strainer and washed with cold RPMI-1640 containing 5mM EDTA. For mouse ear draining lymph nodes cell suspensions, ear draining lymph nodes were mechanically disrupted and passed through a 70-μm strainer. For mouse splenic cell suspensions, spleens were mechanically disrupted and passed through a 70-μm strainer. Cells were then subjected to red blood cell lysis and washed with Phosphate-buffered saline (PBS). Human PBMCs were isolated by density gradient centrifugation using Ficoll paque (GE Healthcare, USA)

In vitro cell stimulation

Mouse splenic cells and human PBMCs were cultured in cell culture media which was altered to pH 6.0 and 7.0 using HCl and NaOH. Cells were stimulated with 100ng/mL PMA (Sigma) and 1μg/mL ionomycin (Sigma) for 4 hours.

Flow cytometry

Cells were resuspended with FACS buffer (phosphate buffered saline containing 2% FCS and 4mM EDTA) and incubated in FcR blocking reagent, mouse (Miltenyi Biotec, Auburn, CA) to block nonspecific antibody binding. For T cells analysis, cell surface staining was conducted for 30 minutes using the following analysis panel: anti-mouse CD45 AF700 (30-F11, BD Pharmingen, San Jose, CA), anti-mouse CD3e PE-Cy7 (145–2C11, BD Pharmingen), anti-mouse TCRβ BV421 (H57–597, BD Horizon), anti-mouse TCRγδ APC (GL3, BioLegend, San Diego, CA), anti-mouse CD4 BV510 (RM4–5, BD Horizon), anti-mouse CD8α PE (53–6.7, BD Pharmingen). For myeloid cell analysis, cell surface staining was conducted for 30 minutes using the following analysis panel: anti-mouse CD45 AF700, anti-mouse CD11b APC (M1/70, BD Pharmingen), anti-mouse Siglec-f BV421 (E50–2440, BD Horizon), anti-mouse Ly6G PE (1A8, BD Pharmingen), anti-mouse

FcεR1α BV510 (MAR-1, BioLegend), anti-mouse c-kit BUV395 (2B8, BD Horizon), anti-mouse CD49b PE-Cy7 (DX5, Invitrogen eBioscience). Dead cells were excluded using 7-AAD (BD, San Jose, CA). Cell counts were determined using flow cytometry counting beads (CountBright Absolute; Life Technologies) following manufacturer instructions. For intracellular cytokine staining, stimulated mouse splenic cells were harvested and surface stained with anti-mouse CD4 Pacific Blue (RM4–5, BD Pharmingen), anti-mouse CD8α AF700 (53–6.7, BD Pharmingen); stimulated human PBMCs were harvested and incubated in Zombie Green fixable viability dye (BioLegend); human cells were then incubated in FcR blocking reagent, human (Miltenyi Biotec) and surface stained with anti-human CD45 AF700 (2D1, Biolegend), anti-human TCRα/β BV510 (BioLegend), anti-human CD4 PE-Cy7 (IP26, BioLegend), anti-human CD8α APC (HIT8α, Biolegend). Cells were then fixed and permeabilized using a Foxp3/Transcription Factor Staining Buffer Set (eBioscience™). Mouse cells were then stained with anti-mouse TNFα PE-Cy7 (MP6-XT22, BioLegend); Human cells were then stained with anti-human TNFα BV421 (MAb11, BioLegend) Sample data were acquired using a 5-laser BD LSRFortessa X-20 flow cytometer and BD FACSDiva software (BD Biosciences) and analyzed using FlowJo software (Tree Star).

Neutrophil Chemotaxis

Neutrophils were isolated from bone marrow as previously described[29]. Briefly, bone marrow was subject to red blood cell lysis and filtered. Neutrophils were purified by gradient density centrifugation. Neutrophils were resuspended in complete media at pH 7.4 or 6.5. 3×10^5 neutrophils were added to the top wells of a transwell plate (Corning). The bottom wells contained complete media with 0, 0.3nM, 1nM or 3nM recombinant CXCL8 (574202, BioLegend). Cells were incubated at 37°C for 1.5 hours. Neutrophils in the bottom wells were quantified by flow cytometry.

Statistical analyses

All graphical representation of data was done using Prism 8.2.1 (GraphPad Software, La Jolla, CA). Data was presented as mean ± standard error of the mean. Normality of distribution of continuous data was assessed by Shapiro-Wilk test. Comparison between multiple groups of different treatments and different mouse strains was analyzed using two-way analysis of variance with Tukey's multiple comparisons test. Comparison between two groups was analyzed using independent two-tailed Student's *t* tests. *P* values less than 0.05 were considered significant. Details of statistical analysis for each experiment can be found in the figure legend (including test details, n, definition of significance, average, and precision metrics)

Results

GPR65 intronic SNP rs8005161 is associated with susceptibility to human AD, IBD and asthma

The T allele of *GPR65* intronic SNP rs8005161 is present at high frequency (~25% in most populations worldwide based on the Ensembl database of 1000 Genomes Phase 3) [30]. The PheWAS for rs8005161 was conducted on 1,228 phenotypes collected from 647,776 genotyped subjects of European ancestry within 23andMe's data set. As reported

by previous studies, rs8005161 showed significant association with inflammatory bowel diseases ($p=3.4\times10^{-5}$) and asthma ($p=3.6\times10^{-5}$) after false discovery rate correction (Fig. 1, Supplemental Table 1). The other major human disease associated with rs8005161 was eczema (atopic dermatitis, AD) ($p=9.2\times10^{-5}$) (Fig. 1, Supplemental Table 1). While the functional validations are abundant for the roles of GPR65 in IBD [7, 8, 31] and asthma [32], the association between GPR65 and AD has never been reported before. However, rs8005161 did not stand out in any existing genome-wide association studies (GWAS) for AD to date [20, 33–35].

Lack of GPR65 signaling exacerbates disease in the murine MC903 atopic dermatitis model

The SNP rs8005161 is in perfect linkage disequilibrium with the GPR65 missense variant rs3742704 (I231L) which results in ~50% less signaling by GPR65, as measured by cAMP production [7]. To investigate the effect of abrogated GPR65 signaling on disease pathogenesis, we studied *Gpr65*$^{gfp/gfp}$ mice that have 90% of an exon in *Gpr65* replaced with green fluorescent protein (GFP) to disrupt GPR65 function [36]. Given the robust correlation between atopic dermatitis and rs8005161, we used a mouse model of AD using MC903 (also known as calcipotriol) (Fig. 2A) to interrogate the effect of GPR65 in the pathogenesis of this disease. Topical application of MC903 induces allergic skin inflammation characterized by pruritic eczematous skin lesions and elevated skin thickness in mice, which highly resembles human AD [37]. *Gpr65*$^{gfp/gfp}$ mice developed exacerbated eczematous skin lesions with far worse ear thickening after MC903 treatment compared to wild-type (WT, C57BL/6) mice (Fig. 2B, 2C, Supplemental Fig. 1A and 1B). Barrier function is considered central in the pathogenesis of AD [38]. We measured the trans-epidermal water loss (TEWL), the loss of water from the skin through the epidermis to the outer environment via diffusion and evaporation processes, to indicate the severity of skin barrier disruption as previously described [39]. *Gpr65*$^{gfp/gfp}$ mice showed significantly higher TEWL than WT mice (Fig. 2D), indicating exacerbated barrier impairment after MC903 treatment. To assess pruritus (itch severity), we counted the times mice scratched their ears over 30 mins on day 14 which was 24 hours prior to the endpoint. In accordance with the severity of disease shown above, *Gpr65*$^{gfp/gfp}$ mice showed higher pruritus (Fig. 2E). Elevated skin pH has been widely reported in AD patients [22–24]. Consistent with this, MC903 treated skin exhibited a significantly higher pH than healthy skin, but there was no difference between WT and *Gpr65*$^{gfp/gfp}$ mice (Fig. 2F). Histopathological assessment demonstrated that the skin of MC903 treated *Gpr65*$^{gfp/gfp}$ mice showed exacerbated inflammation (Fig. 2G) and acanthosis (thickening of the epidermis) (Fig. 2G, 2H). No significant difference was observed in the dermal thickening between WT mice and *Gpr65*$^{gfp/gfp}$ mice (Fig. 2H). Collectively, these data demonstrate that GPR65 deficiency results in exacerbation of AD in a mouse model.

Deficiency of GPR65 increases leukocyte infiltration to inflamed skin

Following the exacerbated phenotypes observed in *Gpr65*$^{gfp/gfp}$ mice, we examined the impact of GPR65 deficiency on leukocyte infiltration in the inflamed site by flow cytometry. As expected, we observed a marked increase of $CD45^{+}$ leukocytes infiltrating the skin and ear draining lymph nodes in *Gpr65*$^{gfp/gfp}$ mice after MC903 treatment, compared to WT

mice (Fig. 3A). Furthermore, we observed significant increases in neutrophils (Fig. 3B) and mast cells (Fig. 3C), and a non-significant increase of basophil infiltration (Supplemental Fig. 3A) in the inflamed skin of *Gpr65*$^{gfp/gfp}$ mice. These subsets are known to contribute to the pathogenesis of AD [40–43]. Eosinophils also play causal roles in AD [44]. However, eosinophil infiltration was slightly reduced in *Gpr65*$^{gfp/gfp}$ mice (Supplemental Fig. 3A). This finding is supported by a previous report on allergic airway disease in mice [32], suggesting that the exacerbation of AD in *Gpr65*$^{gfp/gfp}$ mice is not through eosinophilia.

Effector functions by T cells contributes to the pathogenesis of human AD [15]. Using a rigorous gating strategy for T cells (Supplemental Figure 2), we noticed that GPR65 deficiency results in a drastic elevation of all T cell subsets in inflamed skin, including CD4$^+$ T cells (Fig. 3D), CD8$^+$ T cells (Fig. 3E), and conventional γδ T cells (Fig. 3F). The elevation of T cell numbers caused by GPR65 deficiency was also observed in ear draining lymph nodes (Supplemental Fig. 3B).

GPR65 in humans is expressed mostly by leukocytes, and much less so by epithelial cells [45]. We used the GFP reporter of heterozygous *Gpr65*$^{+/gfp}$ mice to indicate GPR65 expression in different leukocytes infiltrating the inflamed skin. As expected, the reporter GFP was widely detected in cutaneous leukocytes both under resting and inflamed states (Supplemental Fig. 4A). While GPR65 was down-regulated in other leukocytes during MC903-induced inflammation (Supplemental Fig. 4B), it was up-regulated by neutrophils (Fig. 4E, 4F). Collectively, these results suggest that loss of GPR65 increases the presence of inflammatory cells, particularly neutrophils, T cells and mast cells, in the skin after MC903 treatment.

Deficiency of GPR65 also affects neutrophil migration *in vitro*

Neutrophils are highly migratory and pathogenic in several autoimmune inflammatory diseases, including AD [40, 41]. Skin-infiltrating neutrophils are critical for the priming of AD and inducing chronic itch [41]. The application of monoclonal antibodies against the main neutrophil chemokine receptor, CXCR2 can effectively attenuate MC903 atopic dermatitis in mice [46]. Neutrophils express high levels of GPR65 (Fig. 4A, 4B). Protein kinase A (PKA) and cAMP, downstream of GPR65 signaling, play a central role in cytoskeletal re-organization and cell migration [47, 48]. That leukocytes migrate differently with changes in pH was noted more than 20 years ago [49–51]. Compromised GPR65 signaling, for instance by genetic polymorphisms or high pH, may increase leukocyte recruitment to inflamed tissues. We assessed the migratory properties of *Gpr65*$^{gfp/gfp}$ neutrophils towards the neutrophil chemoattractant CXCL8 in an *in vitro* chemotaxis assay at physiological (7.4), and slightly acidic (6.5) pH. Interestingly, the migration of *Gpr65*$^{gfp/gfp}$ neutrophils at either pH was increased compared to WT neutrophils (Fig. 4C), indicating that lack of GPR65 signaling somehow altered the machinery involved in cell migration. Of note, at pH 6.5, WT neutrophil migration was completely inhibited, whereas migration of *Gpr65*$^{gfp/gfp}$ neutrophils was only partially reduced (Fig. 4C). These results demonstrated an inhibitory function of GPR65 in neutrophil migration and the essential anti-inflammatory role of GPR65 signaling at barrier surfaces.

pH and GPR65 regulates TNFα production by CD4+ and CD8+ T cells

From the perspective of adaptive immune responses, cytokine production by T cells is a key factor regulating inflammation. For instance, TNFα is a major inflammatory cytokine, and is easily quantified by intracellular staining. TNFα is elevated the serum of AD patients [52] and plays a causal role in inducing AD-like features on engineered human skin equivalents [27]. Furthermore, TNFα promotes Th2 responses, which is central to the development of AD [53]. GPR65 signaling and cAMP production is known to suppress LPS-induced TNFα production in macrophages [54]. Since we observed a significant increase of T cell infiltration in the skin of *Gpr65*$^{gfp/gfp}$ mice (Fig. 3D–3F), we decided to further understand the influence of pH and GPR65 signaling on T cell functions. We examined intracellular cytokine staining for TNFα in both mouse splenic T cells and human T cells from blood. Acidic pH (pH 6.0) significantly inhibited TNFα production by mouse CD4$^+$ and CD8$^+$ T cells stimulated with phorbol 12-myristate 13-acetate (PMA) (Fig. 4A, 4B). Interestingly, the production of TNFα under acidic pH was partially restored in *Gpr65*$^{gfp/gfp}$ T cells (Fig. 4D, 4E). GPR65 still suppressed TNFα production by CD8$^+$ T cells under neutral pH (pH 7.0) while no difference was observed between WT and *Gpr65*$^{gfp/gfp}$ CD4$^+$ T cells (Fig. 4D, 4E).

To investigate whether the T allele of the rs8005161 polymorphism affects TNFα production by T cells in humans, we identified 6 healthy rs8005161-CT individuals (Chinese Han ancestry, Supplemental Table 2 and 3) and tested the production of TNFα from their T cells from human peripheral blood mononuclear cells (PBMCs) upon PMA/ionomycin stimulation. TNFα production by T cells was also significantly inhibited at pH 6.0 (Fig. 4F and 4G). rs8005161-CT CD4$^+$ T cells produced more TNFα under acidic pH (pH 6.0) compared to rs8005161-CC CD4+ T cells (Fig. 4F and 4G). rs8005161-CT CD8$^+$ T cells showed a non-significant increase of TNFα (Fig. 4F and 4G). We did not identify any rs8005161-TT individuals as these appeared to be rare in the Chinese population under study, despite the large number of CT individuals. Collectively, these data demonstrate that acidity naturally inhibits TNFα production by T cells partially through GPR65, and that the rs8005161 polymorphism is a genetic element that appears to account for variability in cytokine production in human.

Discussion

GPR65 is a receptor that negatively impacts on immune cell responses [1, 2]. This relates to coupling of GPR65 with Gαs, and resulting downstream anti-inflammatory activities [2, 3, 55]. The missense rs3742704 polymorphism (I231L) knocks down cAMP production under acidic pH through GPR65 signaling by ~50%, at least in HeLa cells [7]. We speculated that GPR65 may be extremely important for the regulation of immune responses that would serve to limit immune cell migration or cytokine production, for instance at sites of intense inflammation.

SNPs within *GPR65*, rs3742704 and rs8005161 are associated with IBD [10–13]. Animal studies have shown the involvement of GPR65 in the intestinal and airway inflammations [7–9, 32]. Aligned with these reports, our PheWAS revealed a significant association between *GPR65* SNP rs8005161 and IBD and asthma. Additionally, we found that the

rs8005161 polymorphism in the *GPR65* gene is associated with AD, suggesting a broader influence of GPR65 on barrier responses. Though no existing GWAS for AD supported this association, GPR65 deficiency exacerbated AD phenotypes and led to drier and thicker skin, scalier lesions and compromised barrier integrity in the experimental AD animal model. These results clearly demonstrate a protective role for low pH and GPR65 in AD pathogenesis and, moreover, suggest that PheWAS is able to identify some novel genetic risk loci which did not appear significant in GWAS. AD now adds an important part to a picture: most of the major barriers appear to rely on GPR65 and proton-sensing of low pH for proper homeostasis.

GPR65 is a proton-sensor and is activated under acidic conditions. The pH of normal skin is usually below 6 and can be as low as 4.5 in healthy people [56]. Skin pH in AD patients is often increased into the neutral to basic range [22, 23, 57], a pH where GPR65 signaling is non-operational. This may be important for AD progression because an acidic pH is essential for maintaining skin barrier integrity [21] and normal microbiome composition [57]. Similar to the case in human AD patients, MC903 treatment drastically elevated the skin pH in mice from below 6 to ~ neutral. It is still not fully clear how the skin maintains acidic conditions, but our studies show that low pH is important for proper immune regulation, through GPR65 signaling.

Consistent with the exacerbated AD phenotypes in $Gpr65^{gfp/gfp}$ mice, immune cell infiltration was also significantly elevated in $Gpr65^{gfp/gfp}$ mice after MC903 treatment. These results suggest that GPR65 may regulate AD through immune cell recruitment. While epidermal cells express low levels of GPR65, GPR65 is highly expressed by immune cells [45]. The expression level of GPR65 in most leukocytes was reduced after MC903 treatment and this may result from pH elevation. Increased cell infiltration in $Gpr65^{gfp/gfp}$ mice suggested that GPR65 signaling restricts leukocyte recruitment. It has been largely ignored that pH markedly alters leukocyte migration [49–51] and GPR65 signaling might be the mechanism underlying this. Neutrophils are highly migratory and induce itchiness and scratching during allergic skin inflammation [40, 41]. Notably, neutrophils up-regulated GPR65 during the inflamed state. Moreover, GPR65 signaling inhibited neutrophil migration *in vitro*.

The association of cAMP with cytokine responses led us to investigate whether pH and GPR65 regulate cytokine production by T cells. Acidity inhibited TNFα production by both $CD4^+$ and $CD8^+$ T cells, which was partially dependent on GPR65 in mice. Furthermore, T cells from rs8005161-CT individuals also produced more TNFα compared to T cells from rs8005161-CC individuals, validating the significant anti-inflammatory function of GPR65 in humans. Though, the cohort of participants lacks ethnical diversity, our findings align with the known anti-inflammatory function of GPR65 [2]. Therefore, we propose that circumstances of low pH, such as lactic acid production, or high amounts of short chain fatty acids in the colon, elicits immune-suppressive responses through GPR65. The normal pH of the skin, and the colon, is ~4.5–6.5 and interestingly these tissues are targets for inflammation in rs8005161-CT individuals, presumably because pH has become dysregulated.

Despite that IBD and AD rarely co-occur clinically, the shared genetic risk loci suggest that they might have a complex genetic relationship. A recent meta-analysis reported a positive association between AD and IBD [58], further supporting our findings. GPR65 might be a critical bridge linking the crosstalk between the homeostasis on both major epithelial tissues. AD is the first step of atopic march, which may eventually progress to asthma. AD and asthma both came up in our PheWAS results, suggesting rs8005161 and GPR65 may underly the development of atopic march.

Our study has some limitations. First, our PheWAS was based on self-reported questionnaires which is not as sensitive and specific as a clinical diagnosis. Nevertheless, this was compensated by a large sample size of 647,776 samples. Second, our PheWAS and human experiments are limited by the single ancestry of the cohorts so we are not able to provide the information on the ancestral differences. Third, we acknowledge our findings need to be independently validated in other models of AD, which was outside the scope of the present study.

In conclusion, our study identified an important role for the proton-sensor GPR65 in AD as well as other inflammatory diseases. GPR65 affected processes closely aligned with inflammatory responses, such as cytokine production and cell migration. These findings suggest the possibility of treating AD, IBD and other inflammatory diseases with pH lowering agents or with GPR65 agonists [54, 59].

Supplementary Material

Refer to Web version on PubMed Central for supplementary material.

Acknowledgements

We thank the research participants from 23andMe for their contribution to this study. Members of the 23andMe Research Team: Michelle Agee, Adam Auton, Robert K. Bell, Katarzyna Bryc, Sarah L. Elson, Pierre Fontanillas, Karen E. Huber, Aaron Kleinman, Nadia K. Litterman, Jennifer C. McCreight, Matthew H. McIntyre, Joanna L. Mountain, Elizabeth S. Noblin, Carrie A.M. Northover, Steven J. Pitts, J. Fah Sathirapongsasuti, Olga V. Sazonova, Janie F. Shelton, Suyash Shringarpure, Chao Tian, Joyce Y. Tung, and Vladimir Vacic.

This work was supported by Australian National Health and Medical Research Council (NHMRC).

REFERENCES

1. Okajima F, Regulation of inflammation by extracellular acidification and proton-sensing GPCRs. Cell Signal, 2013. 25(11): p. 2263–71. [PubMed: 23917207]
2. Robert R and Mackay CR, Galphas-coupled GPCRs GPR65 and GPR174. Downers for immune responses. Immunol Cell Biol, 2018. 96(4): p. 341–343. [PubMed: 29542190]
3. Wen AY, Sakamoto KM, and Miller LS, The role of the transcription factor CREB in immune function. J Immunol, 2010. 185(11): p. 6413–9. [PubMed: 21084670]
4. Mogi C, et al. , Involvement of proton-sensing TDAG8 in extracellular acidification-induced inhibition of proinflammatory cytokine production in peritoneal macrophages. J Immunol, 2009. 182(5): p. 3243–51. [PubMed: 19234222]
5. He XD, et al. , Involvement of proton-sensing receptor TDAG8 in the anti-inflammatory actions of dexamethasone in peritoneal macrophages. Biochem Biophys Res Commun, 2011. 415(4): p. 627–31. [PubMed: 22074830]

6. Jin Y, et al. , Inhibition of interleukin-1beta production by extracellular acidification through the TDAG8/cAMP pathway in mouse microglia. J Neurochem, 2014. 129(4): p. 683–95. [PubMed: 24447140]
7. Lassen KG, et al. , Genetic Coding Variant in GPR65 Alters Lysosomal pH and Links Lysosomal Dysfunction with Colitis Risk. Immunity, 2016. 44(6): p. 1392–405. [PubMed: 27287411]
8. Tcymbarevich I, et al. , Lack of the pH-sensing Receptor TDAG8 [GPR65] in Macrophages Plays a Detrimental Role in Murine Models of Inflammatory Bowel Disease. J Crohns Colitis, 2018.
9. Tsurumaki H, et al. , Protective Role of Proton-Sensing TDAG8 in Lipopolysaccharide-Induced Acute Lung Injury. Int J Mol Sci, 2015. 16(12): p. 28931–42. [PubMed: 26690120]
10. Franke A, et al. , Genome-wide meta-analysis increases to 71 the number of confirmed Crohn's disease susceptibility loci. Nat Genet, 2010. 42(12): p. 1118–1125. [PubMed: 21102463]
11. Ke X, Presence of multiple independent effects in risk loci of common complex human diseases. Am J Hum Genet, 2012. 91(1): p. 185–92. [PubMed: 22770979]
12. Ballester V, et al. , Association of NOD2 and IL23R with inflammatory bowel disease in Puerto Rico. PLoS One, 2014. 9(9): p. e108204. [PubMed: 25259511]
13. Liu JZ, et al. , Association analyses identify 38 susceptibility loci for inflammatory bowel disease and highlight shared genetic risk across populations. Nature Genetics, 2015. 47(9): p. 979–986. [PubMed: 26192919]
14. Bieber T, Atopic Dermatitis. Ann Dermatol, 2010. 22(2): p. 125–137. [PubMed: 20548901]
15. Dainichi T, et al. , The epithelial immune microenvironment (EIME) in atopic dermatitis and psoriasis. Nat Immunol, 2018. 19(12): p. 1286–1298. [PubMed: 30446754]
16. Weidinger S and Novak N, Atopic dermatitis. The Lancet, 2016. 387(10023): p. 1109–1122.
17. Larsen FS, Atopic dermatitis: A genetic-epidemiologic study in a population-based twin sample. Journal of the American Academy of Dermatology, 1993. 28(5, Part 1): p. 719–723. [PubMed: 8496415]
18. Larsen PR, Tests related to thyroid hormones in blood: thyroid hormone concentrations. The Thyroid: A Fundamental and Clinical Text, 1986: p. 487–489.
19. Brown SJ, What Have We Learned from GWAS for Atopic Dermatitis? Journal of Investigative Dermatology, 2020.
20. Paternoster L, et al. , Multi-ancestry genome-wide association study of 21,000 cases and 95,000 controls identifies new risk loci for atopic dermatitis. Nature Genetics, 2015. 47(12): p. 1449–1456. [PubMed: 26482879]
21. Schmid-Wendtner MH and Korting HC, The pH of the skin surface and its impact on the barrier function. Skin Pharmacol Physiol, 2006. 19(6): p. 296–302. [PubMed: 16864974]
22. Sparavigna A, Setaro M, and Gualandri V, Cutaneous pH in children affected by atopic dermatitis and in healthy children: a multicenter study. Skin Research and Technology, 1999. 5(4): p. 221–227.
23. Eberlein-Konig B, et al. , Skin surface pH, stratum corneum hydration, trans-epidermal water loss and skin roughness related to atopic eczema and skin dryness in a population of primary school children. Acta Derm Venereol, 2000. 80(3): p. 188–91. [PubMed: 10954209]
24. Angelova-Fischer I, et al. , Skin barrier integrity and natural moisturising factor levels after cumulative dermal exposure to alkaline agents in atopic dermatitis. Acta Derm Venereol, 2014. 94(6): p. 640–4. [PubMed: 24531413]
25. Lee HJ, et al. , Topical acidic cream prevents the development of atopic dermatitis- and asthma-like lesions in murine model. Exp Dermatol, 2014. 23(10): p. 736–41. [PubMed: 25078153]
26. Lee NR, et al. , Application of Topical Acids Improves Atopic Dermatitis in Murine Model by Enhancement of Skin Barrier Functions Regardless of the Origin of Acids. Ann Dermatol, 2016. 28(6): p. 690–696. [PubMed: 27904267]
27. Danso MO, et al. , TNF-α and Th2 Cytokines Induce Atopic Dermatitis–Like Features on Epidermal Differentiation Proteins and Stratum Corneum Lipids in Human Skin Equivalents. Journal of Investigative Dermatology, 2014. 134(7): p. 1941–1950.

28. Radu CG, et al. , Differential proton sensitivity of related G protein-coupled receptors T cell death-associated gene 8 and G2A expressed in immune cells. Proc Natl Acad Sci U S A, 2005. 102(5): p. 1632–7. [PubMed: 15665078]
29. Swamydas M and Lionakis MS, Isolation, Purification and Labeling of Mouse Bone Marrow Neutrophils for Functional Studies and Adoptive Transfer Experiments. J Vis Exp, 2013(77): p. 50586.
30. Cunningham F, et al. , Ensembl 2019. Nucleic Acids Res, 2019. 47(D1): p. D745–d751. [PubMed: 30407521]
31. Tcymbarevich IV, et al. , The impact of the rs8005161 polymorphism on G protein-coupled receptor GPR65 (TDAG8) pH-associated activation in intestinal inflammation. BMC Gastroenterol, 2019. 19(1): p. 2. [PubMed: 30616622]
32. Kottyan LC, et al. , Eosinophil viability is increased by acidic pH in a cAMP- and GPR65-dependent manner. Blood, 2009. 114(13): p. 2774–82. [PubMed: 19641187]
33. Hirota T, et al. , Genome-wide association study identifies eight new susceptibility loci for atopic dermatitis in the Japanese population. Nature Genetics, 2012. 44(11): p. 1222–1226. [PubMed: 23042114]
34. Ferreira MA, et al. , Shared genetic origin of asthma, hay fever and eczema elucidates allergic disease biology. Nature Genetics, 2017. 49(12): p. 1752–1757. [PubMed: 29083406]
35. Ferreira MAR, et al. , Eleven loci with new reproducible genetic associations with allergic disease risk. Journal of Allergy and Clinical Immunology, 2019. 143(2): p. 691–699.
36. Radu CG, et al. , Normal immune development and glucocorticoid-induced thymocyte apoptosis in mice deficient for the T-cell death-associated gene 8 receptor. Mol Cell Biol, 2006. 26(2): p. 668–77. [PubMed: 16382156]
37. Li M, et al. , Topical vitamin D3 and low-calcemic analogs induce thymic stromal lymphopoietin in mouse keratinocytes and trigger an atopic dermatitis. Proc Natl Acad Sci U S A, 2006. 103(31): p. 11736–41. [PubMed: 16880407]
38. Kabashima K, New concept of the pathogenesis of atopic dermatitis: Interplay among the barrier, allergy, and pruritus as a trinity. Journal of Dermatological Science, 2013. 70(1): p. 3–11. [PubMed: 23473856]
39. Holm EA, et al. , Instrumental assessment of atopic eczema: Validation of transepidermal water loss, stratum corneum hydration, erythema, scaling, and edema. Journal of the American Academy of Dermatology, 2006. 55(5): p. 772–780. [PubMed: 17052481]
40. Oyoshi MK, et al. , Leukotriene B4-driven neutrophil recruitment to the skin is essential for allergic skin inflammation. Immunity, 2012. 37(4): p. 747–58. [PubMed: 23063331]
41. Walsh CM, et al. , Neutrophils promote CXCR3-dependent itch in the development of atopic dermatitis. Elife, 2019. 8.
42. Liu F-T, Goodarzi H, and Chen H-Y, IgE, Mast Cells, and Eosinophils in Atopic Dermatitis. Clinical Reviews in Allergy & Immunology, 2011. 41(3): p. 298–310. [PubMed: 21249468]
43. Siracusa MC, et al. , Basophils and allergic inflammation. Journal of Allergy and Clinical Immunology, 2013. 132(4): p. 789–801.
44. Naidoo K, et al. , Eosinophils Determine Dermal Thickening and Water Loss in an MC903 Model of Atopic Dermatitis. Journal of Investigative Dermatology, 2018. 138(12): p. 2606–2616.
45. Uhlen M, et al. , Proteomics. Tissue-based map of the human proteome. Science, 2015. 347(6220): p. 1260419. [PubMed: 25613900]
46. Alam MJ, et al. , Therapeutic blockade of CXCR2 rapidly clears inflammation in arthritis and atopic dermatitis models: demonstration with surrogate and humanized antibodies. MAbs, 2020. 12(1): p. 1856460. [PubMed: 33347356]
47. Howe AK, Regulation of actin-based cell migration by cAMP/PKA. Biochim Biophys Acta, 2004. 1692(2–3): p. 159–74. [PubMed: 15246685]
48. Mosenden R and Tasken K, Cyclic AMP-mediated immune regulation--overview of mechanisms of action in T cells. Cell Signal, 2011. 23(6): p. 1009–16. [PubMed: 21130867]
49. Rotstein OD, et al. , The deleterious effect of reduced pH and hypoxia on neutrophil migration in vitro. Journal of Surgical Research, 1988. 45(3): p. 298–303.

50. Simchowitz L and Cragoe EJ Jr., Regulation of human neutrophil chemotaxis by intracellular pH. J Biol Chem, 1986. 261(14): p. 6492–500. [PubMed: 3009458]

51. Bryant RE, et al. , Studies on human leukocyte motility. I. Effects of alterations in pH, electrolyte concentration, and phagocytosis on leukocyte migration, adhesiveness, and aggregation. J Exp Med, 1966. 124(3): p. 483–99. [PubMed: 4958802]

52. Sumimoto S, et al. , Increased plasma tumour necrosis factor-alpha concentration in atopic dermatitis. Archives of Disease in Childhood, 1992. 67(3): p. 277. [PubMed: 1575548]

53. Choi JP, et al. , TNF-alpha is a key mediator in the development of Th2 cell response to inhaled allergens induced by a viral PAMP double-stranded RNA. Allergy, 2012. 67(9): p. 1138–1148. [PubMed: 22765163]

54. Onozawa Y, et al. , Activation of T cell death-associated gene 8 regulates the cytokine production of T cells and macrophages in vitro. Eur J Pharmacol, 2012. 683(1–3): p. 325–31. [PubMed: 22445881]

55. Hershko DD, et al. , Multiple transcription factors regulating the IL-6 gene are activated by cAMP in cultured Caco-2 cells. Am J Physiol Regul Integr Comp Physiol, 2002. 283(5): p. R1140–8. [PubMed: 12376407]

56. Lambers H, et al. , Natural skin surface pH is on average below 5, which is beneficial for its resident flora. Int J Cosmet Sci, 2006. 28(5): p. 359–70. [PubMed: 18489300]

57. Panther DJ and Jacob SE, The Importance of Acidification in Atopic Eczema: An Underexplored Avenue for Treatment. J Clin Med, 2015. 4(5): p. 970–8. [PubMed: 26239459]

58. Lee H, et al. , Bidirectional relationship between atopic dermatitis and inflammatory bowel disease: A systematic review and meta-analysis. Journal of the American Academy of Dermatology, 2020. 83(5): p. 1385–1394. [PubMed: 32497689]

59. Huang XP, et al. , Allosteric ligands for the pharmacologically dark receptors GPR68 and GPR65. Nature, 2015. 527(7579): p. 477–83. [PubMed: 26550826]

Key points

1. *GPR65* intronic SNP rs8005161 is associated with the risk of atopic dermatitis.
2. GPR65 deficient mice developed exacerbated atopic dermatitis in an animal model.
3. pH and GPR65 signaling regulate neutrophil migration and TNFα production by T cells.

A

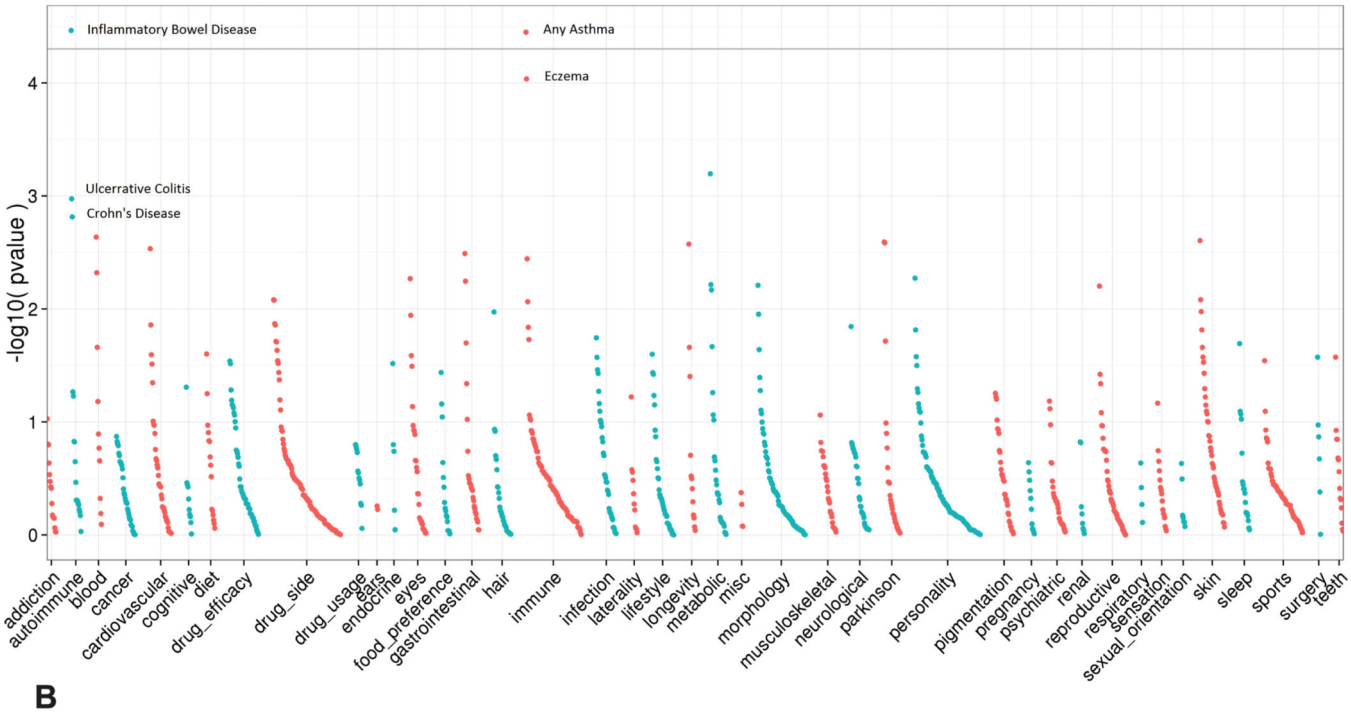

B

Phenotypes	Odd Ratio (95% CI)	P Value	FDR
Crohn's or Ulcerative colitis	1.10 (1.05-1.15)	3.44E-05	0.021842777
Any asthma	1.05 (1.02-1.07)	3.55E-05	0.021842777
Eczema	1.04 (1.02-1.07)	9.22E-05	0.037778755

Figure 1. *GPR65* intronic SNP rs8005161 associates with human atopic dermatitis.

(A) A forest plot summarising the association effects of rs8005161 on a set of selected phenotypes from PheWAS in 23andMe. Phenotypes are arranged by their broad phenotypic categories along the X-axis. Y-axis represents log-scaled P values. Positions with $P < 5 \times 10^{-5}$ (a score of about 4.3) are shown in grey, which is a threshold for significance after controlling for the Family-Wise-Error-Rate (FWER) using Bonferroni correction. The vertical scale is adjusted nonlinearly (log scaled) to preserve detail for signals near the genome-wide threshold. The selected phenotypes include significant association of Eczema, IBD and Asthma. Additional selected phenotypes include other immune diseases, any cancer, and any infections.

(B) A table summarizing the top association effects of rs8005161 from PheWAS in 23andMe. CI, confidence interval. FDR, False discovery rate.

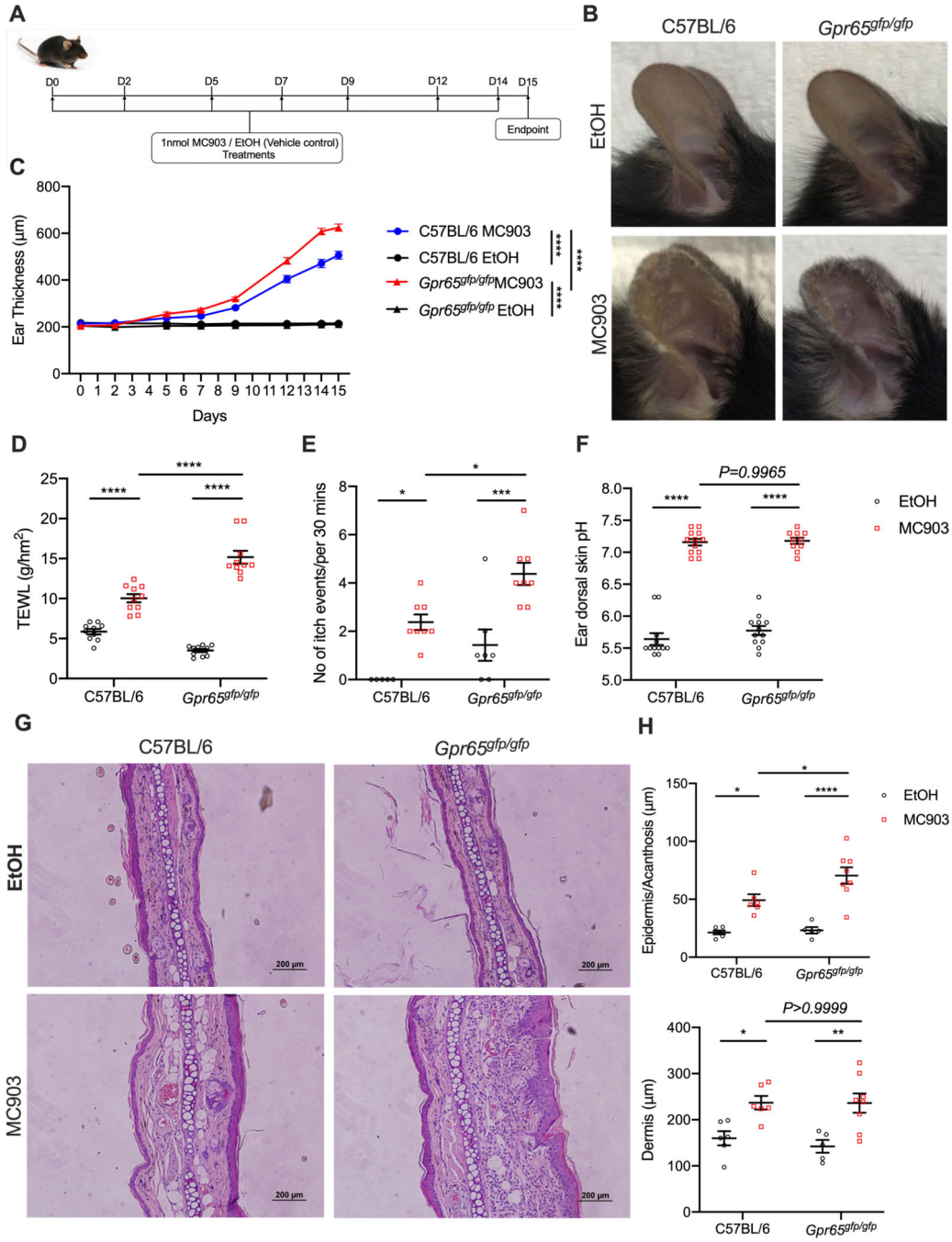

Figure 2. GPR65 deficiency exacerbates mouse MC903-induced AD phenotypes.

(A) Scheme of the experimental treatment regimen.

(B) Representative appearance of EtOH and MC903 treated ears of C57BL/6 and *Gpr65*$^{gfp/gfp}$ mice at the endpoint.

(C) Ear thickness at each treatment day.

(D) TEWL at the endpoint.

(E) Ear itch assessment at day 14 (24 hours prior the endpoint).

(F) Ear dorsal skin pH at day 14.

(G) Representative ear sections stained with hematoxylin and eosin EtOH and MC903 treated ears of C57BL/6 and *Gpr65*$^{gfp/gfp}$ mice. Original magnification = × 400, scale bar = 200μm.

(H) Acanthosis (Epidermal thickening) and dermal thickening.

Each graph is representative of at least three independent experiments. Each data point represents an individual ear or mouse, and n = 6–8 mice in each group. All data represented as means ± SEM. Two-way analysis of variance with Tukey posttest. *P < 0.05, **P < 0.01, ***P < 0.005, ****P < 0.0001. EtOH, ethanol. TEWL, trans-epidermal water loss.

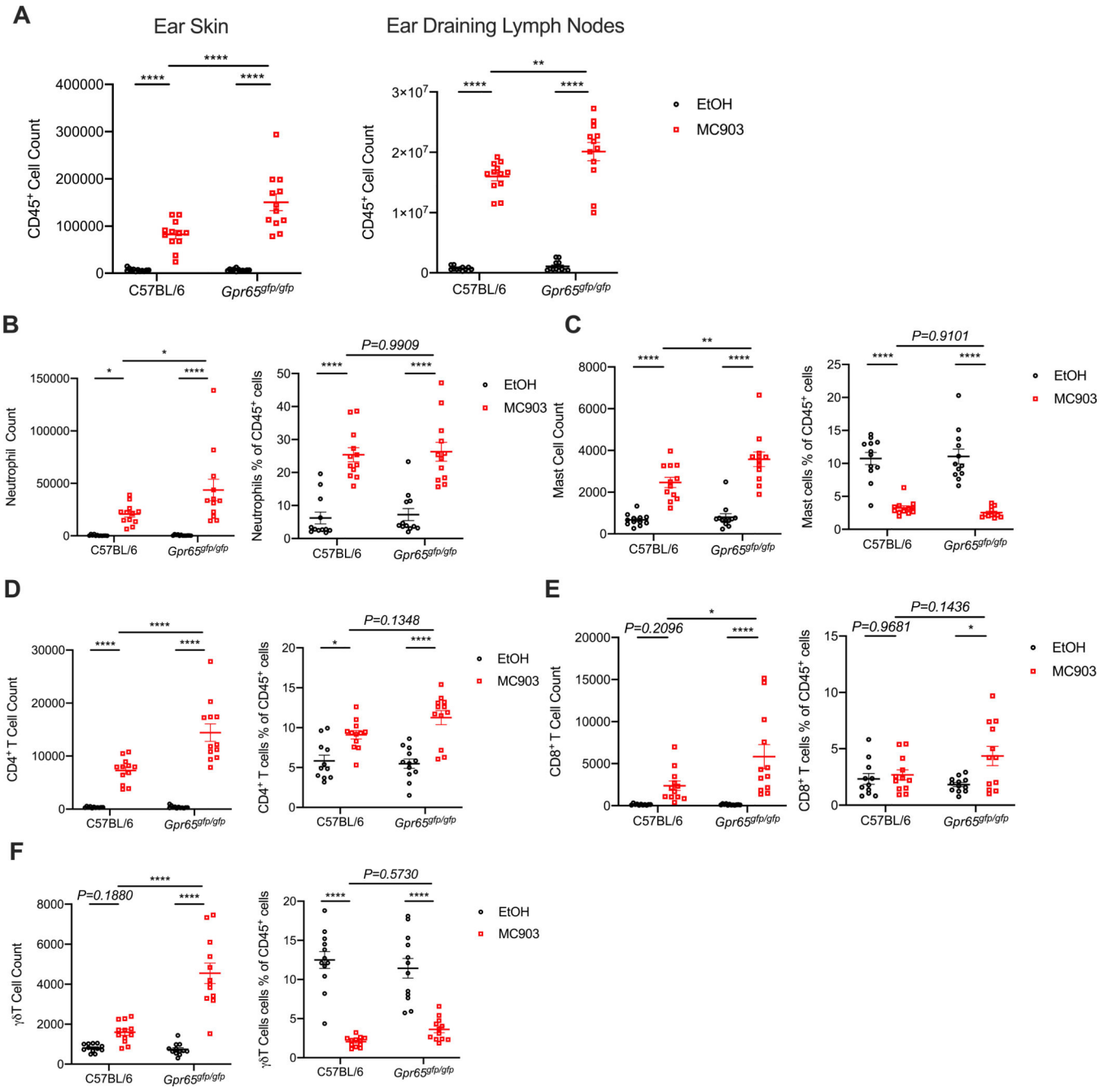

Figure 3. GPR65 deficiency increases leukocyte infiltration in mouse MC903-induced AD.

(A) Count of $CD45^+$ leukocytes from total cells in skin and in ear draining lymph nodes. (B)-(F) Count and percentage of neutrophils (B), mast cells (C), $CD4^+$ T cells (D), $CD8^+$ T cells (E) and γδT cells (F) from $CD45^+$ leukocytes in skin.

Each graph is summarized from least three independent experiments. Each data point represents an individual mouse, and n = 11–12 mice in each group. All data represented as means ± SEM. Two-way analysis of variance with Tukey posttest. *P < 0.05, **P < 0.01, ***P < 0.005, ****P < 0.0001. EtOH, ethanol.

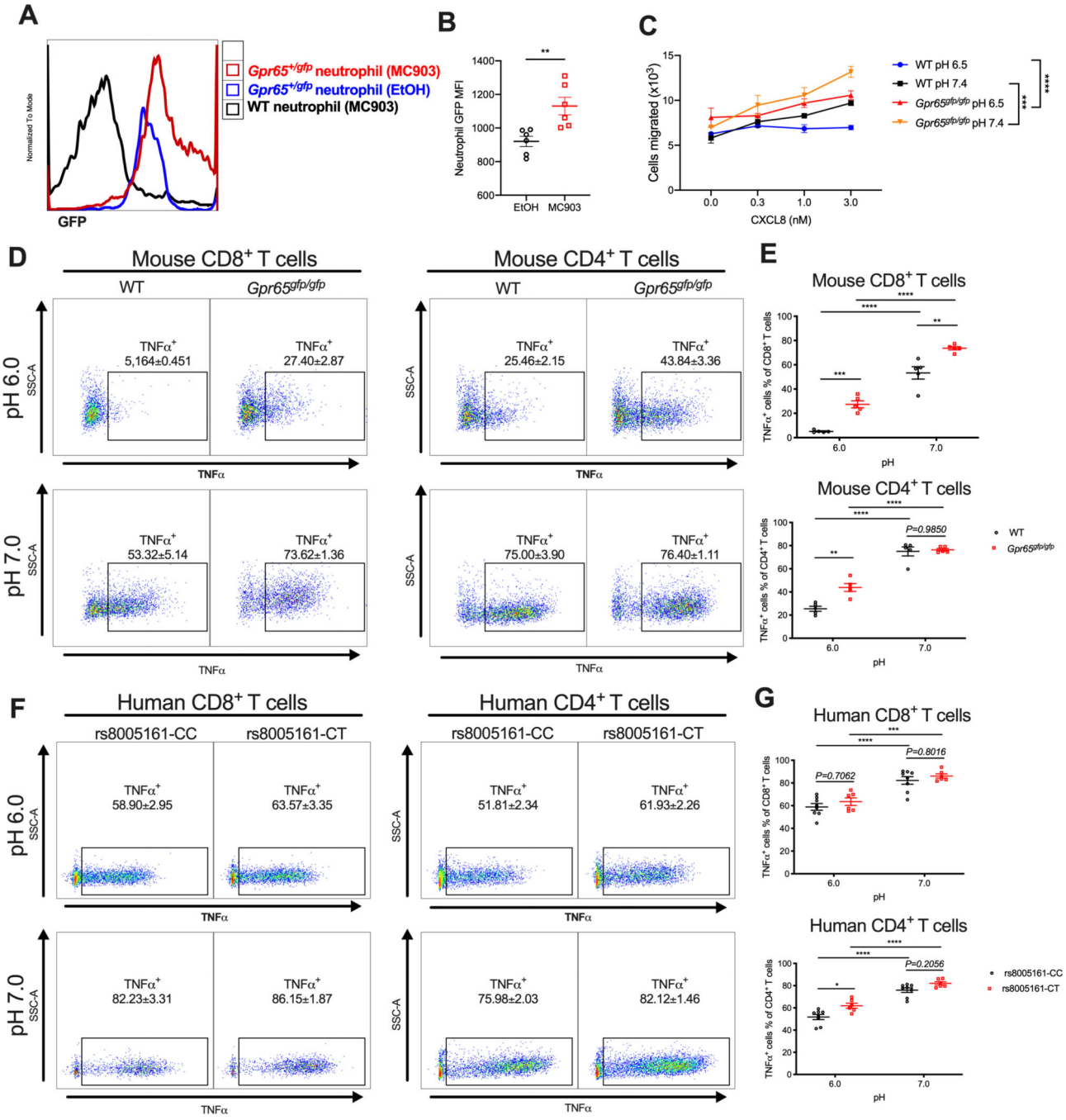

Figure 4. Acidic pH regulated AD-related immunity in a GPR65 dependent way in both mice and human.

(A) Representative GFP reporter histogram of neutrophils from ear skin of C57BL/6 and *Gpr65*$^{gfp/+}$ mice treated with EtOH or 1nmol MC903.

(B) Median fluorescence intensity (MFI) of GFP reporter in neutrophils of *Gpr65*$^{gfp/+}$ mice. Each graph is representative of at least three independent experiments. Each data point represents an individual mouse, and n = 6 mice in each group. Unpaired two-tailed t test.

(C) Assessment of neutrophil chemotaxis towards CXCL8. The number of neutrophils that migrated across a transwell membrane was determined by flow cytometry. Each graph

is representative of at least three independent experiments. n=3 replicates in each group. Two-way analysis of variance with Tukey posttest.

(D)-(G) 1×10^6 cells/well of splenic leukocytes from naïve C57BL/6 and *Gpr65*$^{gfp/gfp}$ mice or 1×10^6 cells/well of human peripheral mononuclear cells (PBMCs) from rs8005161-CC and rs8005161-CT individuals were stimulated with 100ng/mL PMA and 1μg/mL ionomycin at the presence of 10μg/mL Brefeldin A (BFA) at pH 6.0 and 7.0 for 4 hours. (D) Representative pseudocolor plots for TNFα producing WT and *Gpr65*$^{gfp/gfp}$ $CD8^+$ T cells and $CD4^+$ T cells at pH 6.0 and 7.0 (Gated from $CD8^+$ T cells and $CD4^+$ T cells). (E) Percentage of TNFα producing $CD8^+$ T cells and $CD4^+$ T cells at pH 6.0 and 7.0 among WT and *Gpr65*$^{gfp/gfp}$ cells. (F) Representative pseudocolor plots for TNFα producing rs8005161-CC and rs8005161-CT $CD8^+$ T cells and $CD4^+$ T cells at pH 6.0 and 7.0 (Gated from $CD8^+$ T cells and $CD4^+$ T cells). (G) Percentage of TNFα producing $CD8^+$ T cells and $CD4^+$ T cells at pH 6.0 and 7.0 among rs8005161-CC and rs8005161-CT cells. Each graph is representative of at least three independent experiments. Two-way analysis of variance with Tukey posttest.

All data represented as means ± SEM. *P < 0.05, **P < 0.01, ***P < 0.005, ****P < 0.0001.